Available online at www.sciencedirect.com

ScienceDirect

Scripta Materialia 87 (2014) 49–52

Scripta MATERIALIA

www.elsevier.com/locate/scriptamat

Estimation of the Hall–Petch strengthening coefficient of steels through nanoindentation

Moo-Young Seok,[a] In-Chul Choi,[a] Joonoh Moon,[b] Sungju Kim,[c] Upadrasta Ramamurty[d,e] and Jae-il Jang[a,*]

[a]*Division of Materials Science and Engineering, Hanyang University, Seoul 133-791, Republic of Korea*
[b]*Ferrous Alloys Research Group, Korea Institute of Materials Science, Changwon 641-831, Republic of Korea*
[c]*R&D Center, Sheet Products Design Team, Hyundai Steel Company, Dangjin 343-823, Republic of Korea*
[d]*Department of Materials Engineering, Indian Institute of Science, Bangalore 560012, India*
[e]*Center of Excellence for Advanced Materials Research, King Abdulaziz University, Jeddah 21589, Saudi Arabia*

Received 22 March 2014; revised 13 May 2014; accepted 13 May 2014
Available online 20 May 2014

A method to estimate the Hall–Petch coefficient k for yield strength and flow stress of steels through nanoindentation experiments is proposed. While determination of k_f for flow stress is on the basis of grain boundary strengthening evaluated by sharp indentation, k_y for yield strength was computed with pop-in data from spherical indentations. Good agreement between estimated and literature data, obtained from the tensile tests, validates the proposed methodology.

Keywords: Steel; Hall–Petch relation; Nanoindentation; Grain boundary strengthening

One of the most important microstructural parameters that control the yield strength, σ_y, of polycrystalline metals and alloys is the grain size, d [1]. At the beginning of 1950s, Hall [2] and Petch [3] independently observed that σ_y scales with $d^{-0.5}$ in a number of metals and alloys. On this basis, the widely known Hall–Petch (HP) relation is derived:

$$\sigma_y = (\sigma_y)_0 + k_y d^{-\frac{1}{2}} \quad (1)$$

where $(\sigma_y)_0$ is the friction stress free from grain boundary (GB) contributions (and thus is approximately the σ_y of an extremely coarse-grained, untextured polycrystal) and k_y is a material constant, which is often referred to as the "HP coefficient" or the "locking parameter". Note that in alloys with different microstructural constituents, such as α/β Ti alloy with grains, colonies and laths, d can be replaced by the deformation-controlling microstructural length scale; the functional form of Eq. (1) is still obeyed [4]. Later, it was suggested that the flow stress at any given strain $\sigma(\varepsilon)$ also obeys the HP relation [1,5]:

$$\sigma(\varepsilon) = \sigma_0(\varepsilon) + k_f d^{-\frac{1}{2}} \quad (2)$$

where $\sigma_0(\varepsilon)$ corresponds to the flow stress of single crystal at that strain and k_f is the HP coefficient for flow stress. Similarly, it was reported that the HP equation can successfully describe the grain size effect on hardness, H, albeit with a different k [5].

The HP coefficient is an important indicator of the relative contribution of GBs to the strength of the material. If k is small – as in Ti alloys, for example – the strength enhancement that one can obtain through grain refinement may not be much and other alloy design principles may have to be invoked for strengthening the alloy. Usually, the experimental evaluation of k of a material is performed through a series of standard tensile tests on samples with varying d, and some values of k for σ_y are listed in Table 1 [2,6–13]. However, this procedure requires a large amount of material as several tests on many standard-sized samples with different grain sizes are essential for a complete study.

* Corresponding author. Tel.: +82 222200402; fax: +82 222202294; e-mail: jijang@hanyang.ac.kr

http://dx.doi.org/10.1016/j.scriptamat.2014.05.004
1359-6462/

Table 1. Hall–Petch coefficient k_y measured from tensile tests in previous studies [2,6–13].

Type of steel	k_y (MPa·mm$^{1/2}$)	Ref.
Mild steel	19.05	[2]
Mild steel	17.42	[6]
Plain carbon steel (0.034C)	25.6	[7]
Plain carbon steel (0.07C)	27.97	
Low-carbon steel	17.9	[8]
Ultrahigh-carbon steel	14.55	[9]
Mild steel	23.40	[10]
Swedish iron	22.45	
Cr steel	18.97	[11]
Mild steel	18	[12]
Ferritic steel	18.97	[13]

To circumvent this, we suggest in this paper a simple methodology that utilizes the nanoindentation technique, and demonstrate it on two different steels. A clear advantage of the suggested method is that one can estimate the values of k for $\sigma(\varepsilon)$ as well as σ_y independently using only a small volume of material. In this context, we recognize that some literature on utilizing the nanoindentation technique for evaluating the GB contribution to the strengthening in metals and alloys exists, especially for thin films [14–19]. Soer et al. [20,21], for example, proposed that k_y could be estimated from the nanoindentation data obtained with a blunt tip. However, methodologies that offer ways to estimate k_y and k_f separately are not yet available. Recently, Seok et al. [22] have suggested a way to predict the overall strength of dual-phase steels from the data obtained by nanoindenting individual phases. In that work, strengthening due to GBs was considered, but only in a qualitative manner. With this in mind, a simple methodology for estimating both k_y and k_f, where the GB contribution is accounted for in a quantitative manner, is proposed and validated in the present paper.

Two types of steel were examined in this study: a commercial-grade API X70 linepipe steel (with a nominal composition (in wt.%) of Fe–0.07C–0.2Si–1.55Mn–0.07Nb–0.04V–0.02Ti) and a low-carbon steel (composition (in wt.%) Fe–0.07C–1.2Mn–0.15Si). Both of these alloys have a two-phase microstructure consisting of ferrite and pearlite. All specimens were mechanically polished with fine SiC paper up to grit number 2000, then electrolytically polished using a Lectropol-5 instrument (Struers, Westlake, OH) in an 80% ethanol/14% distilled water/6% perchloric acid solution to avoid artifacts related to a hardened surface layer that can be introduced during grinding. Specimens were etched with 3% Nital solution for microstructure observations by an optical microscope (Olympus, Tokyo, Japan). The grain size and volume fraction of each microstructural phase were measured with an Image-Pro image analyzer (Media Cybernetics Inc., Silver Springs, MD).

Nanoindentation tests were carried out under the continuous stiffness measurement (CSM) module of the Nanoindenter-XP (formerly MTS; now Agilent Technologies, Oak Ridge, TN) at a constant indentation strain rate $(dP/dt)/P$ (where P is the indentation load) of 0.05 s^{-1} with either a three-sided pyramidal Berkovich indenter or a spherical indenter. The values of hardness (H) were estimated according to the procedure outlined by Oliver and Pharr [23]. Before performing the spherical indentation tests, the tip radius, R, was determined as ~3.43 μm through calibration tests on fused quartz utilizing the Hertzian contact theory [24]. Subsequently, grid indentations were performed on electropolished samples.

The samples were etched subsequent to the indentation experiments, and scanning electron microscopy and electron backscatter diffraction (EBSD) with an FEI XL30 FEG instrument (Philips, Cambridge, UK) were performed so as to assign each indent to either of the phases or the inter-phase or GB regions. In the current work we did not consider the influence of each grain's crystallographic orientation on H as it is not significantly affected by the orientation [25].

First, the k_f of Eq. (2) for API X70 steel was estimated using the results of the nanoindentation experiments with a Berkovich indenter. Representative load–displacement (P–h) responses obtained for each phase of the steel are shown in Figure 1. It is apparent in Figure 1a that the peak load displacement (h_{max}) is much larger in the softer ferrite than in the pearlite. The measured H values are summarized in Figure 1b, and are in a reasonable agreement with the literature data [15,26]. With the well-known Tabor's empirical relationship [27], $\sigma = H/C$, where C is the constraint factor (~3 for fully plastic deformation [27]), k_f of Eq. (2) can be determined from:

$$k_f \cdot d^{-\frac{1}{2}} = \sigma(\varepsilon) - \sigma_0(\varepsilon) = \Delta\sigma_{GB} \sim \frac{\Delta H_{GB}}{3} \tag{3}$$

where $\Delta\sigma_{GB}$ and ΔH_{GB} are the GB strengthening contributions to $\sigma(\varepsilon)$ and H, respectively. ΔH_{GB} may be determined by a simple rule-of-mixture of the phase hardness data:

$$\Delta H_{GB} = (H_{macro})_{exp} - \{(H_0)_F(1 - f_P) + (H_0)_P f_P\} \tag{4}$$

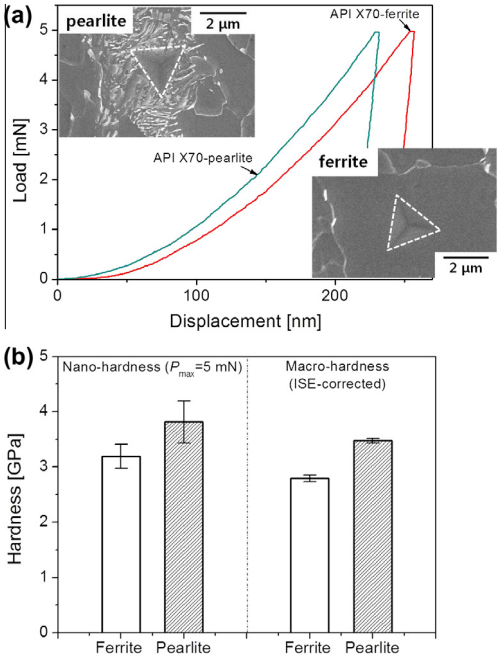

Figure 1. Results of nanohardness measurements for API X70 steel; (a) representative P–h curves for each phase (with inset images showing hardness impressions); (b) obtained hardness of each phase.

where $(H_{\mathrm{macro}})_{\mathrm{exp}}$ is the H obtained from high-load indentation (in this study, $P_{\max} = 500$ mN) so that it includes the GB strengthening effect, H_0 is the H corresponding to $\sigma_0(\varepsilon)$ of Eqs. (2) and (3), f is the volume fraction of each phase within the indentation-induced plastic zone, and subscripts F and P indicate ferrite and pearlite, respectively. The first and second terms in Eq. (4) are H with and without GB contributions, respectively.

To determine f_{P} of Eq. (4), a scratch was made on the polished specimen as a reference, and the regions adjoining it were imaged before (Fig. 2a) and after nanoindentation tests (Fig. 2b). For the sake of simplicity, the area of the indentation-induced plastic zone was assumed to be the same as that of the circle passing three (or at least two) angular points of the triangular hardness impression. An example of the image taken using an image analyzer is provided in the inset of Figure 2b, the white and black areas of which correspond to the ferrite and pearlite phases, respectively. The value of f_{P} can be calculated from such an image (e.g. $f_{\mathrm{P}} = 0.1205$ for the inset of Fig. 2b), and f_{F} can be also simply determined as $(1 - f_{\mathrm{P}})$. The average f_{P} in the microstructure of API X70 steel is ~6%.

Since the phase hardness values, $(H_0)_{\mathrm{P}}$ and $(H_0)_{\mathrm{F}}$ of Eq. (4), were obtained at a relatively low load (for this study, 5 mN) and $(H_{\mathrm{macro}})_{\mathrm{exp}}$ was measured at a high load (500 mN), they cannot be directly compared to each other due to the indentation size effect (ISE), i.e. an increase in H with decreasing h for a sharp indenter [28]. To take ISE into account, the following Nix–Gao equation can be used [28]:

$$(H_{macro})_{ISE} = H\left(\sqrt{1+\frac{h^*}{h}}\right)^{-1} \quad (5)$$

where $(H_{\mathrm{macro}})_{\mathrm{ISE}}$ is the ISE-corrected macroscopic hardness estimated by Eq. (5) and h^* is a material length scale for h-dependent H. Figure 1b also provides the $(H_{\mathrm{macro}})_{\mathrm{ISE}}$ of each phase. With the measured data of H and f, k_{f} can be computed according to Eqs. (3) and (4). The estimated ΔH_{GB} was ~0.1843 GPa and thus k_{f} was ~3.60 MPa·mm$^{1/2}$.

Since the estimated k_{f} is for both ferrite–ferrite and ferrite–pearlite boundaries, we attempted again to estimate k_{f} for only ferrite–ferrite boundaries of this steel through nanoindentation tests on the ferrite-only area (where f_{P} is ~0), as shown in Figure 2c and d. Using the procedure described above, the computed values for ferrite–ferrite boundaries were $\Delta H_{\mathrm{GB}} = 0.177$ GPa and hence $k_{\mathrm{f}} = \sim 3.45$ MPa·mm$^{1/2}$. The similarity in both the values of k_{f} suggests that the strengthening due to high-angle GBs is independent of the neighboring phases and depends exclusively on the matrix microstructure (including dislocation density) and chemical compositions.

Next, we attempted to estimate k_{y} of Eq. (1) through spherical indentation on a low-carbon steel, which was selected instead of API X70 for the following two reasons: (i) it has considerably larger average d, which allows for the demarcation of the indents on the GB and on grain interior (GI); and (ii) the high initial dislocation density in API X70 makes the detection of the first pop-in, which is the key indicator for elastic-to-plastic transition of deformation underneath the indenter [29–31], difficult. During spherical nanoindentation, the P–h curves often exhibit a sudden burst of h, at a constant P in the case of load-controlled tests, which is often referred to as pop-in. The maximum shear stress at the first pop-in, $\tau_{\max}$, represents the critical shear strength for the onset of plasticity and hence can be related to σ_{y}.

Figure 3 shows representative P–h curves exhibiting pop-ins for the indentations of GBs and GIs. The inset is an EBSD image showing the region where nanoindentations were performed. The indentations marked by dashed circle correspond to the P–h curves of GBs. The average pop-in load for the GBs is lower than that of GIs, which is opposite to the typical expectation that GBs are harder than GIs [16,32]. This can be explained by the different natures hardness and pop-in behavior, being similar to the difference between k_{f} and k_{y}; hardness is governed by interactions between moving dislocations and crystalline defects (e.g. the GBs and other dislocations) and hence is enhanced by the presence of the GBs. In contrast, the pop-in behavior is controlled

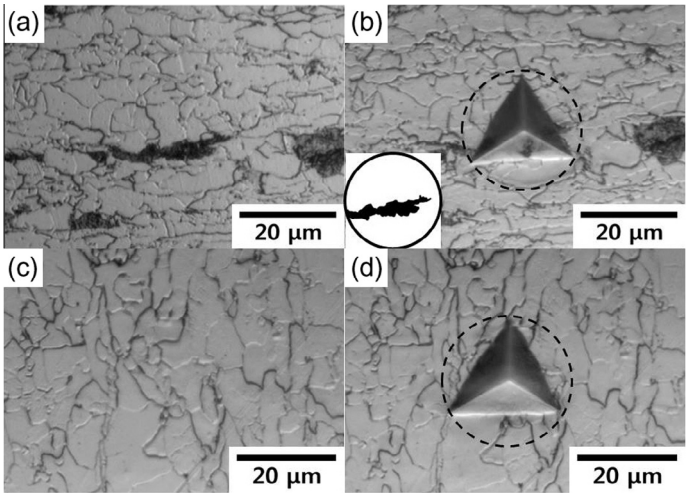

Figure 2. Optical micrographs taken before (a, c) and after (b, d) high-load nanoindentation tests ($P_{\max} = 500$ mN) (a, b) for a two-phase region and (c, d) for a ferrite-only region.

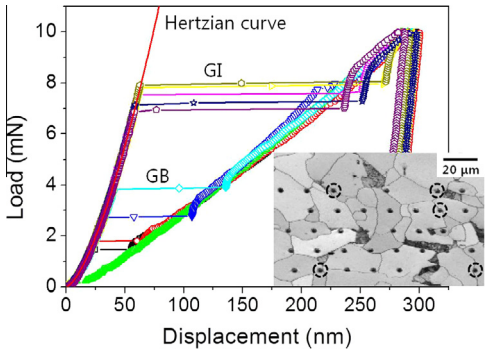

Figure 3. Pop-in behavior observed in the *P–h* curves of spherical indentations. The inset image is the corresponding EBSD map showing which one is made on GBs (marked by a dashed circle).

either by the dislocation nucleation or bursts in dislocation movements, and hence can occur at lower P when the indentation is performed in the vicinity of a GB, as GBs can act as a source for dislocation nucleation [33].

In spherical indentation, τ_{max} occurs at a distance approximately half the contact radius directly below the rotational axis of the contact and is given by [34]:

$$\tau_{max} = 0.31 \cdot p_0 = 0.31 \cdot \left(\frac{3}{2} p_m\right) = 0.31 \cdot \left(\frac{6 \cdot P_P \cdot E_r^2}{\pi^3 \cdot R^2}\right)^{\frac{1}{3}} \quad (6)$$

where p_0 and p_m are the maximum and mean pressures of the contact, respectively, and P_P and E_r are the first pop-in load and the reduced modulus. In consideration of the GB's role as an effective barrier for the passage of dislocations, yielding occurs when the stress at the tip of the dislocation pile-up reaches the critical value, τ_c, necessary to nucleate slip across the GB. Based on this scenario, Eq. (1) can be rewritten as [33,34]:

$$\sigma_y = (\sigma_y)_0 + k_y d^{-\frac{1}{2}} = (\sigma_y)_0 + M\sqrt{\frac{2\tau_c Gb}{A\pi}} \cdot d^{-\frac{1}{2}}. \quad (7)$$

Here M is the Taylor factor, G is the shear modulus, b the Burgers vector and A is a constant equal to $(1 - \nu)$ or 1 for edge or screw dislocations, respectively, where ν is Poisson's ratio. Based on the GB's role as an obstacle of dislocation movement, it is reasonable to assume that. if pop-in occurs during the indentation on a GB, the critical stress τ_c in Eq. (7) is equal to the maximum shear stress τ_{max}. By considering the τ_c of Eq. (7) as the same as the obtained τ_{max} (~1.7–4.2 GPa), k_y was estimated as $\sim 19.68 \pm 3.20$ MPa·mm$^{1/2}$, which is in reasonable agreement with the literature data [2,6–13] listed in Table 1. It can also be noted from Table 1 that k_y does not vary significantly between various types of steel.

In summary, we demonstrate a simple methodology to estimate the Hall–Petch coefficient k for yield strength and flow stress of a steel through nanoindentation experiments. While k_f was estimated on the basis of hardening due to GBs, which was evaluated with the aid of a simple rule-of-mixture and ISE theory, k_y was evaluated with the "pop-in" data from spherical indentation. Estimated values are in reasonable agreement with the literature data.

This research was supported in part by the National Research Foundation of Korea (NRF) grant funded by the Korea government (MSIP) (No. 2013R1A1A2A10058551), and in part by the Human Resources Development program of the Korea Institute of Energy Technology Evaluation and Planning (KETEP) grant funded by the Korea government (MOTIE) (No. 20134030200360).

[1] N. Hansen, Scr. Mater. 51 (2004) 801.
[2] E.O. Hall, Proc. R. Soc. B 64 (1951) 747.
[3] N.J. Petch, J. Iron Steel Inst. 174 (1953) 25.
[4] I. Sen, S. Tamirasakandala, D. Miracle, U. Ramamurty, Acta Mater. 55 (2007) 4983.
[5] R.W. Armstrong, Metall. Trans. 1 (1970) 1169.
[6] W.B. Morrison, Trans. ASM 59 (1966) 824.
[7] P.H. Chang, A.G. Preban, Acta Metall. 33 (1985) 897.
[8] H. Asahi, A. Yagi, M. Ueno, ISIJ Inter. 33 (1993) 1190.
[9] C.K. Syn, D.R. Lesuer, O.D. Sherby, Metall. Mater. Trans. A 25A (1994) 1481.
[10] M.A. Meyers, K.K. Chawla, Mechanical Behavior of Materials, Prentice-Hall, Engleweood Cliffs, NJ, 1999.
[11] Y. Funakawa, T. Ujiro, ISIJ Inter. 50 (2010) 1488.
[12] A. Ramazani, K. Mukherjee, U. Prahl, W. Bleck, Metal. Mater. Trans. A 43A (2012) 3850.
[13] S. Takaki, Mater. Sci. Forum 706 (2012) 181.
[14] J.-I. Jang, S. Shim, S.-I. Komazaki, T. Honda, J. Mat. Res. 22 (2007) 175.
[15] B.-W. Choi, D.-H. Seo, J. Jang, Metal. Mater. Int. 15 (2009) 373.
[16] T. Ohmura, L. Zhang, K. Sekido, K. Tsuzaki, J. Mater. Res. 27 (2012) 1742.
[17] W.A. Soer, J.Th.M. De Hosson, A.M. Minor, J.W. Morris Jr., E.A. Stach, Acta Mater. 52 (2004) 5783.
[18] W.A. Soer, J.Th.M. De Hosson, A.M. Minor, Z. Shan, S.A. Syed Asif, O.L. Warren, Appl. Phys. Lett. 90 (2007) 181924.
[19] K.E. Aifantis, W.A. Soer, J.Th.M. De Hosson, J.R. Willis, Acta Mater. 54 (2006) 5077.
[20] W.A. Soer, K.E. Aifantis, J.Th.M. De Hosson, Acta Mater. 53 (2005) 4665.
[21] W.A. Soer, J.Th.M. De Hosson, Mater. Lett. 59 (2005) 3192.
[22] M.-Y. Seok, Y.-J. Kim, I.-C. Choi, Y. Zhao, J.-I. Jang, Int. J. Plast. (2014), http://dx.doi.org/10.1016/j.ijplas.2014.03.013.
[23] W.C. Oliver, G.M. Pharr, J. Mater. Res. 7 (1992) 1564.
[24] K.L. Johnson, Contact Mechanics, Cambridge University Press, Cambridge, 1985.
[25] J.J. Vlassak, W.D. Nix, J. Mech. Phys. Solids 42 (1994) 1223.
[26] R. Rodriguez, I. Gutierrez, Mater. Sci. Eng. A 361 (2003) 377.
[27] I.-C. Choi, Y.-J. Kim, Y.M. Wang, U. Ramamurty, J.-I. Jang, Acta Mater. 61 (2013) 7313.
[28] G.M. Pharr, E.G. Herbert, Y. Gao, Annu. Rev. Mater. Res. 40 (2010) 271.
[29] I.-C. Choi, Y. Zhao, B.-G. Yoo, Y.-J. Kim, J.-Y. Suh, U. Ramamurty, J.-I. Jang, Scr. Mater. 66 (2012) 923.
[30] J.-I. Jang, H. Bei, P.F. Becher, G.M. Pharr, J. Am. Ceram. Soc. 95 (2012) 2113.
[31] I.-C. Choi, Y. Zhao, Y.-J. Kim, B.-G. Yoo, J.-Y. Suh, U. Ramamurty, J.-I. Jang, Acta Mater. 60 (2012) 6862.
[32] Y. Zhao, I.-C. Choi, Y.-J. Kim, J.-I. Jang, J. Alloys Compd. 582 (2014) 141.
[33] J.P. Hirth, J. Lothe, Theory of Dislocations, Krieger, Malabar, FL, 1992.
[34] N. Hansen, Mater. Sci. Eng. A 4009 (2005) 39.